Correlation effects and concomitant two-orbital $s_\pm$-wave superconductivity in $La_3Ni_2O_7$ under high pressure

Yi-Heng Tian,[*] Yin Chen,[*] Jia-Ming Wang,[*] Rong-Qiang He,[†] and Zhong-Yi Lu[‡]
Department of Physics, Renmin University of China, Beijing 100872, China
and Key Laboratory of Quantum State Construction and Manipulation (Ministry of Education), Renmin University of China, Beijing 100872, China

(Received 15 December 2023; accepted 9 April 2024; published 26 April 2024)

High-T_c superconductivity (SC) has been found experimentally in the bilayer material $La_3Ni_2O_7$ under high pressure recently, in which the Ni-$3d_{3z^2-r^2}$ and $3d_{x^2-y^2}$ orbitals are expected to play a key role in the electronic structure and the SC. Here we study the two-orbital electron correlations and the nature of the SC in the framework of the dynamical mean-field theory using the bilayer two-orbital Hubbard model downfolded from the band structure of $La_3Ni_2O_7$. We find that each of the two orbitals forms $s_\pm$-wave SC pairing. Because of the interorbital hoppings, the two-orbital SCs are concomitant, and furthermore they transition to Mott insulating states simultaneously when tuning the system to half filling. The Hund's coupling induced local interorbital spin coupling enhances the electron correlations pronouncedly and is crucial to the SC.

DOI: 10.1103/PhysRevB.109.165154

I. INTRODUCTION

After being studied for more than three decades, the superconducting (SC) mechanism of cuprates as the first class of unconventional high-temperature superconductors remains elusive [1]. While undoped cuprates are antiferromagnetic Mott insulators, in doped cuprates the SC takes place in the CuO_2 layer and shows $d_{x^2-y^2}$-wave symmetry. In-plane antiferromagnetic spin correlations are thought to be crucial for the Cooper pairing. Because of the large Coulomb interaction of the active Cu-$3d_{x^2-y^2}$ orbital, cuprates are strongly electronically correlated. Doped cuprates are thought of as doped Mott insulators [2–4] and are usually described by a single-band Hubbard or t-J model in theoretical studies. Besides cuprates, there are other SC strongly correlated electronic materials being discovered [5–7].

Recently, the bilayer Ruddlesden-Popper phased $La_3Ni_2O_7$ under high pressure was found to be another high-temperature superconductor [8] and quickly attracted a lot of attention [9–36]. Reminiscent of the CuO_6 octahedra in cuprates, the bilayer stacked NiO_6 octahedra are the key structure for the SC. Like cuprates, the $La_3Ni_2O_7$ features a linear resistivity behavior in the high-temperature normal state, implying that its normal state is a strange metal and it may be a strongly correlated electronic material. As the density functional theory (DFT) based band structure calculations [8] show, the three Ni-t_{2g} orbitals are fully filled while the two e_g orbitals are partially filled and hence active for the low-energy physics. Bridged by the apical oxygen p_z orbital in the middle of the bilayer, the Ni-$3d_{3z^2-r^2}$ orbital in the top layer and that in the bottom layer have a large effective hopping and form a low-energy σ-bonding state and a high-energy antibonding state. This is absent for the Cu-$3d_{x^2-y^2}$ cuprates. The interplay between the two e_g orbitals and the bilayer structure may lead to new electron correlation behaviors and different SC mechanisms.

Angle-resolved photoemission spectroscopy (ARPES) experiments at ambient pressure [33] and some theoretical studies [10,12,13,17,19,34] have indicated that the two e_g orbitals in the Ni atoms exhibit orbital-selective characteristics. The electronic correlation in the Ni-$3d_{3z^2-r^2}$ orbitals are stronger than that in the Ni-$3d_{x^2-y^2}$ orbitals. Furthermore, many theoretical studies have indicated that under high pressure the leading pairing symmetry for the SC is of $s_\pm$ wave [11,14,15,22,24,26–28,34–36], and factors like the Hund's coupling [24,25,27,28] and the Ni-$3d_{3z^2-r^2}$ orbital's effective interlayer antiferromagnetic coupling [20,24,26,27,29,35,36] could be crucial for the SC. These interactions are evident in a dimer composed of two vertically aligned Ni atoms, suggesting that studying the pairing mechanism of high-pressure $La_3Ni_2O_7$ through the lens of a dimer may be fruitful.

In this paper, we study the bilayer two-orbital model [37] describing the $La_3Ni_2O_7$ under high pressure, including the most two relevant correlated orbitals, namely the Ni-$3d_{3z^2-r^2}$ (denoted as z) and $3d_{x^2-y^2}$ (denoted as x) orbitals. The model is solved by (cellular) dynamical mean-field theory (DMFT) [38,39] at zero temperature. We analyze the relation between the two orbitals and find that they are orthogonal but correlated, which gives rise to concomitant two-orbital SC or Mott states. Orbital selective Mott (or SC) phases can emerge out only when suppressing the interorbital hoppings. When doping away from half filling, the ground state is a two-orbital $s_\pm$-wave SC, where the z-orbital SC is weaker than the x-orbital SC. To study the effect of the local interorbital spin correlation on the SC, we define an effective local interorbital

[*]These authors contributed equally to this work.
[†]rqhe@ruc.edu.cn
[‡]zlu@ruc.edu.cn

spin coupling (LIOSC) split from the Hund's coupling [40]. We find that the LIOSC enhances significantly the electron correlations and makes the z-orbital interlayer antiferromagnetic correlation shared with the x orbitals to help the x-orbital Cooper pairing.

II. MODEL AND METHOD

We employ the bilayer two-orbital model proposed in Ref. [37], which was obtained by the Wannier downfolding of the DFT band structure. Each layer is a square lattice. One layer is staked on top of the other. The unit cell contains one site on the top layer and one site in the bottom layer. Each site contains both e_g orbitals. The Hamiltonian is

$$\begin{aligned} H &= H_0 + H_I, \\ H_0 &= \sum_{\mathrm{k}\sigma} \Psi^\dagger_{\mathrm{k}\sigma} H(\mathrm{k}) \Psi_{\mathrm{k}\sigma}, \\ H_I &= U \sum_{il\alpha} \left(n_{il\alpha\uparrow} - \frac{1}{2}\right)\left(n_{il\alpha\downarrow} - \frac{1}{2}\right) \\ &\quad + U'_{\mathrm{a}} \sum_{il\sigma} \left(n_{ilx\sigma} - \frac{1}{2}\right)\left(n_{ilz\bar{\sigma}} - \frac{1}{2}\right) \\ &\quad + U'_{\mathrm{p}} \sum_{il\sigma} \left(n_{ilx\sigma} - \frac{1}{2}\right)\left(n_{ilz\sigma} - \frac{1}{2}\right), \end{aligned} \tag{1}$$

where $\Psi_\sigma = (d_{Ax\sigma}, d_{Az\sigma}, d_{Bx\sigma}, d_{Bz\sigma})^T$ and $d_{s\sigma}$ annihilates an $s = Ax, Az, Bx, Bz$ electron with spin σ. A and B label the top layer and the bottom layer, x and z label $d_{x^2-y^2}$ and $d_{3z^2-r^2}$ orbitals, respectively. The lattice is shown in Fig. 2(a) of Ref. [37] while the model parameters are listed in Table I of Ref. [37]. By convention, we set $U'_{\mathrm{a}} = U - 2J$, $U'_{\mathrm{p}} = U - 3J$, and $J = U/4$, where J is the Hund's coupling. $U'_{\mathrm{a}}(U'_{\mathrm{p}})$ is the interorbital repulsion strength for antiparallel (parallel) spins. We choose $U = 4$ eV with eV being the energy unit. We further add a chemical potential to the Hamiltonian (1) for electron density tuning. The band structure and Fermi surface of H_0 is shown in Fig. 3 of Ref. [37].

Because of the mirror symmetry of the model, it is convenient to transform to the bonding (+) and antibonding (−) states for both e_g orbitals $\Psi_{\pm\mathrm{k}\sigma} = (c_{x\pm\mathrm{k}\sigma}, c_{z\pm\mathrm{k}\sigma})^T$ with $c_{\alpha\pm\mathrm{k}\sigma} = d_{\alpha\mathrm{kA}\sigma} \pm d_{\alpha\mathrm{kB}\sigma}$, in which the Hamiltonian becomes block diagonal.

We solve this bilayer two-orbital model with (cellular) DMFT [38,39] at zero temperature. The DMFT self-consistently maps the original model to a quantum impurity model. In this paper, the impurity consists of two sites within a unit cell of the original lattice. So the local quantum fluctuation and interlayer quantum correlation have been fully considered. By using the irreducible representation [41,42], our impurity model ensures the equivalence of the two layers. Local and interlayer SC electron pairings between antiparallel spins are both allowed, while in-plane nonlocal SC pairings, including d-wave pairings, are not considered in our method. We have calculated the bonding and antibonding SC pairing order parameters

$$\Delta_{\alpha\pm} = \langle c_{\alpha\pm\uparrow} c_{\alpha\pm\downarrow} \rangle \tag{2}$$

as well as the local and interlayer SC pairing order parameters,

$$\begin{aligned} \Delta_{0\alpha} &= \langle d_{A\alpha\uparrow} d_{A\alpha\downarrow} \rangle = \langle d_{B\alpha\uparrow} d_{B\alpha\downarrow} \rangle, \\ \Delta_{1\alpha} &= \tfrac{1}{2} \langle d_{A\alpha\uparrow} d_{B\alpha\downarrow} + d_{B\alpha\uparrow} d_{A\alpha\downarrow} \rangle, \end{aligned} \tag{3}$$

where $\alpha = x, z$ labels different orbitals. Note that $\Delta_{\alpha\pm} = \Delta_{0\alpha} \pm \Delta_{1\alpha}$.

The electronic bath for the quantum impurity model is discretized into a number of bath sites. Then the quantum impurity model is solved by exact diagonalization (ED) [43] and natural orbital renormalization group (NORG) [44–46] methods. The ED method can treat at most eight bath sites and is used for most calculations. The NORG method can treat 12 bath sites so that the bath is better described, which is adopted for the calculation for Fig. 4.

III. RESULTS AND DISCUSSION

A. Orthogonality and hybridization between the two e_g orbitals

An electron can hop from a z orbital of a Ni atom (say, the atom at the origin) to an x orbital of its nearby Ni atoms via t_3^{xz} and t_4^{xz}, and further to other orbitals of other Ni atoms. But it will never hop to the x orbitals of the original Ni atom and the other Ni atom (in the other layer) in the same unit cell and all the Ni atoms along the diagonal sites of the lattice. This is forbidden by the symmetry and quantum destructive interference. All possible hopping paths will exactly and destructively interfere because, after a mirror operation against the $x = y$ plane, the x orbitals change signs while the z orbitals do not. As a result, on the $x = y$ plane (especially in a unit cell) there are no hybridization and Cooper pairings between the two e_g orbitals, i.e., they are orthogonal to each other.

However, orthogonality does not mean independence. Fluctuations in the z orbitals induce fluctuations in the x orbitals, and vice versa, because of the interorbital hoppings t_3^{xz} and t_4^{xz} [47,48]. As a result, the two e_g orbitals are simultaneously SC or Mott insulating. One can not suppress SC in one orbital while leaving the other SC. And one orbital takes a Mott transition only when the other does simultaneously. In this aspect, the two e_g orbitals correlate with each other [47].

B. Simultaneous Mott transition of the two e_g orbitals

As we increase the chemical potential μ, the electron densities of the two orbitals grow gradually. The electron density of z orbitals (n_z) reaches half-filling first. But the z orbitals do not encounter a Mott transition here because the x orbitals are away from half-filling and can not be Mott insulating. As we further increase μ, n_z even surpasses one and then drops back to one as n_x grows to one, as shown in the inset of Fig. 1(a). Then the two orbitals take a Mott transition simultaneously (Fig. 1), the SC disappears (Fig. 2), and both the electron densities become constant [Fig. 1(a)]. In other words, there are no orbital selective Mott transitions (OSMT) in the two e_g orbitals. The phenomenon of the absence of OSMT due to interorbital hopping has been studied in [48]. Interorbital hopping allows electrons to hop through an intermediate orbital, breaking the Mott insulating state that would otherwise characterize these orbitals. The phenomenon that we have observed here is similar, with the x orbital serving as

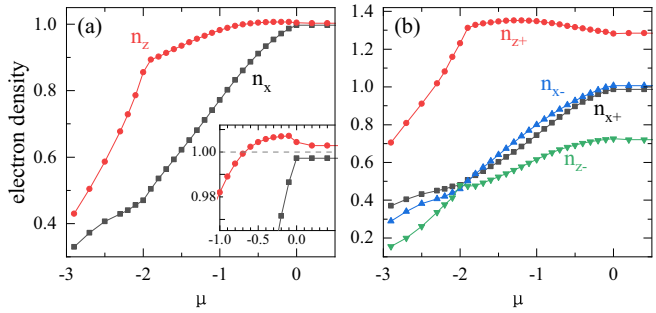

FIG. 1. Electron density of a Ni atom as a function of the chemical potential μ. (a) Electron densities for different orbitals. Inset: enlarged view around half-filling. When $\mu > -2$, the increase of n_z becomes slow. When μ exceeds -0.7, n_z surpasses one without the z orbitals being Mott insulating. As n_x gradually approaches one, n_z drops back to one, and the two orbitals simultaneously transition from SC to Mott insulating at $\mu = 0$. (b) Electron densities for the bonding and antibonding states of different orbitals. As μ decreases from zero, n_{z+} increases counterintuitively and n_{z-} is not small, implying that the z orbitals are strongly correlated. A negative electronic compressibility is observed on the bonding state of the z orbital.

the intermediate orbital. Its hoppings with the z orbital disrupt the Mott insulating state of the z orbital.

C. Concomitant $s_\pm$-wave SCs

When doping away from half-filling, the ground state of the system becomes superconducting. The electrons pair mainly between the two z orbitals, as well as the two x orbitals of the two Ni atoms in a unit cell, namely $\Delta_{1z} \neq 0$ and $\Delta_{1x} \neq 0$, while Δ_{0z} and Δ_{0x} are small [Fig. 2(a)]. Because of the orthogonality between the x orbitals and z orbitals in a unit cell, there are no electron pairings between them. As a result, $\Delta_{z\pm} = \Delta_{0z} \pm \Delta_{1z} \neq 0$ and $\Delta_{x\pm} = \Delta_{0x} \pm \Delta_{1x} \neq 0$ [Fig. 2(b)] but $\langle c_{x\pm\uparrow} c_{z\pm\downarrow} \rangle = 0$, i.e., both of the two e_g orbitals are $s_\pm$-wave pairing, but there are no Cooper pairings between them. Nevertheless, we want to emphasize that, because of the hybridization between the two orbitals, the two $s_\pm$-wave SCs are concomitant and there are no orbital selective SC (OSSC) in the two e_g orbitals.

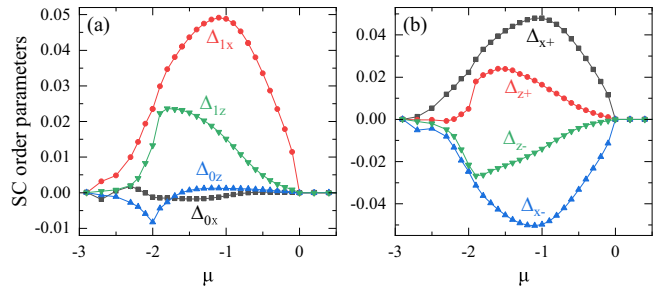

FIG. 2. SC order parameters vs the chemical potential μ. (a) Local ($\Delta_{0\alpha}$) and interlayer ($\Delta_{1\alpha}$) pairings. In the whole SC regime, the interlayer pairing is dominant, and Δ_{1x} is larger than Δ_{1z}. (b) SC order parameters for the bonding ($\Delta_{\alpha+}$) and antibonding ($\Delta_{\alpha-}$) states. Both of the two orbitals are $s_\pm$-wave superconducting and become Mott insulating simultaneously at $\mu = 0$.

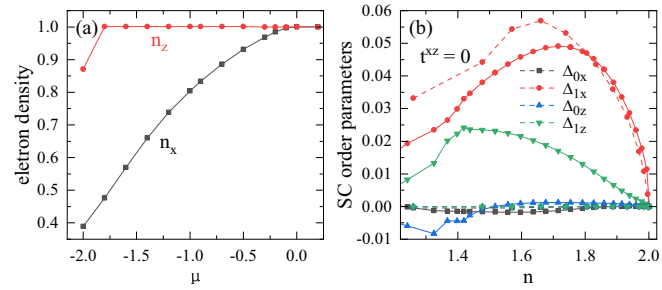

FIG. 3. (a) Electron densities for different orbitals and (b) SC order parameters as functions of chemical potential μ after t_3^{xz} and t_4^{xz} being suppressed to zero. Solid lines represent order parameters for normal hopping parameters, and dashed lines for hopping parameters with t_3^{xz} and t_4^{xz} suppressed to zero. An orbital selective Mott (or SC) phase has been observed after suppressing the interorbital hopping parameters t^{xz}. All SC order parameters have been suppressed except Δ_{1x}.

To show the crucial role of the interorbital hoppings [47,48] for the simultaneous Mott transition and the concomitant $s_\pm$-wave SCs, we do another calculation with them turned off, i.e., setting $t_3^{xz} = t_4^{xz} = 0$. In this case, the two e_g orbitals couple to each other only through the two-body interactions, the interorbital hybridization disappears, and the interorbital charge flow is forbidden. Consequently, we have observed an OSMT and OSSC (Fig. 3), where, as the chemical potential increases, the z orbitals reach half filling first and become Mott insulating, and their SC has been suppressed. In contrast, the x-orbital SC is almost unaffected, which is robust and does not rely on the SC of the z orbitals.

D. Dramatically enhanced electron correlations and the effect on the SC by the local interorbital spin coupling

Strong correlation, especially antiferromagnetic (AFM) spin correlation, induced by the Coulomb interaction is believed to play a key role in unconventional SCs. In $La_3Ni_2O_7$ under high pressure, a strong interlayer AFM correlation between the two z orbitals can be induced by the intraorbital Hubbard interaction and the effective hopping between the two z orbitals mediated by the oxygen-$2p_z$ orbital between them. In contrast, this mechanism is missing for the x-orbital counterpart, but the x-orbital $s_\pm$-wave SC is robust as shown above. A sound explanation for its AFM correlation is that the x orbitals share the AFM correlation of the z orbitals through the Hund's coupling, which tends to align the spins of the two e_g orbitals in a single Ni atom. We study this point in more detail.

To this end, we reformulate the local interorbital interaction in a single site as follows:

$$\sum_\sigma U'_{\rm a} n_{x\sigma} n_{z\bar{\sigma}} + U'_{\rm p} n_{x\sigma} n_{z\sigma} = \frac{U'_{\rm a} + U'_{\rm p}}{2} n_x n_z - 2(U'_{\rm a} - U'_{\rm p}) s_x^z s_z^z, \quad (4)$$

where n_α represents the electron number of the α orbital, and s_α^z denotes the z component of the spin of the α orbital. We define a local interorbital spin coupling (LIOSC) $\Delta U' =$

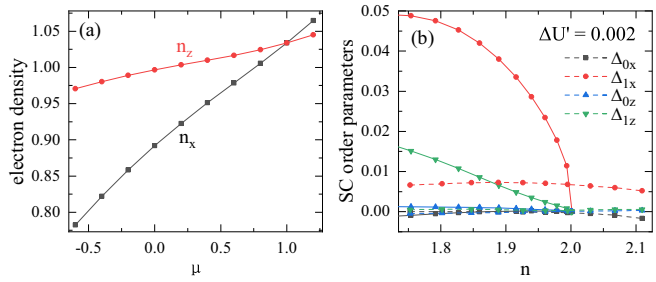

FIG. 4. (a) Electron densities and (b) SC order parameters with $\Delta U' = U'_a - U'_p = 0.002$ and $U'_a + U'_p$ unchanged. An almost linear relation for both n_x and n_z as μ increases. In (b), solid lines represent order parameters for $\Delta U' = 1$ and dashed lines for $\Delta U' = 0.002$. Δ_{1x} has been suppressed to a small magnitude, and other SC order parameters almost disappear.

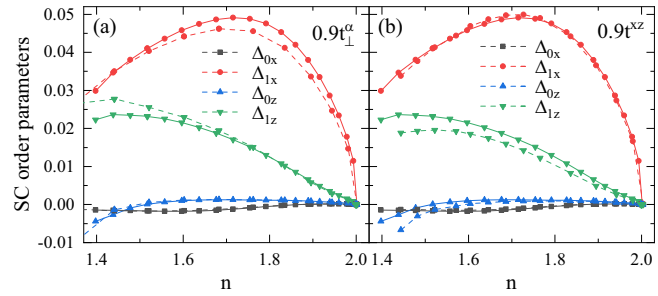

FIG. 5. SC order parameters vs electron density for different values of hopping parameters. Solid lines represent order parameters for normal hopping parameters, and dashed lines for hopping parameters which are suppressed. (a) $t_\perp^\alpha$ for both orbitals being reduced by 10%. (b) t_3^{xz} and t_4^{xz} being reduced by 10%.

$U'_a - U'_p$, which exactly accounts for the spin correlation between the two e_g orbitals in a Ni atom. We do a calculation with reducing $\Delta U'$ from its normal value J to a negligible value $0.002J$ while keeping $(U'_a + U'_p)/2$ unchanged. Surprisingly, the previous Mott insulating state with a large Mott gap disappears [Fig. 4(a)], and the SCs of the two orbitals are greatly suppressed (about seven times weaker for both the two orbitals), showing that the LIOSC $\Delta U'$ can dramatically enhance the electron correlations and is crucial to the high T_c SC for this two-orbital system. This supports the above mechanism.

On the other hand, the interlayer AFM correlation depends directly on the interlayer hoppings $t_\perp^z$ and $t_\perp^x$. Reducing them suppresses the x-orbital SC [Fig. 5(a)], implying that the x-orbital SC relies on the interlayer AFM correlation of the z orbitals. This also supports the above picture.

Although the interlayer AFM correlation for the z orbitals is strong, its SC is weaker than the x-orbital SC. This is because the coherent moving of the z orbital Cooper pairs is more difficult since all the in-plane hoppings for the z orbitals are small. When reducing t_3^{xz} and t_4^{xz}, the z-orbital SC is suppressed while the x-orbital SC is not [Fig. 5(b)].

IV. SUMMARY

To study the correlation effects and the high-T_c SC in $La_3Ni_2O_7$ under high pressure, we have adopted the (cellular) DMFT on a bilayer two-orbital Hubbard model. The two active e_g orbitals and their interlayer correlations are included. We have observed concomitant two-orbital $s_\pm$-wave SC. The two e_g orbitals transition simultaneously from the Mott insulating states at half filling to the $s_\pm$-wave SC states upon tuning the electron density. This phenomenon arises from the unique electronic structure of the system: the two orbitals are orthogonal to each other on the $x = y$ plane due to symmetry and quantum destructive interference, but essentially hybridized due to their interorbital hoppings. The z orbitals form $s_\pm$-wave SC because of their strong interlayer hoppings and antiferromagnetic correlation. But its SC order parameter is not large because of their weak in-plane hoppings. In contrast, the x orbitals form strong $s_\pm$-wave SC by sharing the interlayer antiferromagnetic correlation from that of the z orbitals. This sharing is accounted for by the local interorbital spin correlation caused by the effective local interorbital spin coupling (LIOSC). When suppressing the LIOSC, the Mott state disappears and the SC is suppressed remarkably, implying that the LIOSC enhances pronouncedly the electron correlation and is crucial to the SC. When suppressing the interorbital hoppings, the two orbitals do not correlate with each other anymore and an orbital selective Mott or SC phase has been observed.

ACKNOWLEDGMENTS

This work was supported by the National Natural Science Foundation of China (Grant No. 11934020). Computational resources were provided by the Physical Laboratory of High Performance Computing in Renmin University of China.

[1] B. Keimer, S. A. Kivelson, M. R. Norman, S. Uchida, and J. Zaanen, From quantum matter to high-temperature superconductivity in copper oxides, Nature (London) **518**, 179 (2015).

[2] N. F. Mott, Metal-insulator transition, Rev. Mod. Phys. **40**, 677 (1968).

[3] M. Imada, A. Fujimori, and Y. Tokura, Metal-insulator transitions, Rev. Mod. Phys. **70**, 1039 (1998).

[4] P. A. Lee, N. Nagaosa, and X.-G. Wen, Doping a Mott insulator: Physics of high-temperature superconductivity, Rev. Mod. Phys. **78**, 17 (2006).

[5] Y. Kamihara, T. Watanabe, M. Hirano, and H. Hosono, Iron-based layered superconductor $La[O_{1-x}F_x]FeAs$ ($x = 0.05 - 0.12$) with $T_c = 26$ K, J. Am. Chem. Soc. **130**, 3296 (2008).

[6] A. Chubukov, Pairing mechanism in Fe-based superconductors, Annu. Rev. Condens. Matter Phys. **3**, 57 (2012).

[7] D. Li, K. Lee, B. Y. Wang, M. Osada, S. Crossley, H. R. Lee, Y. Cui, Y. Hikita, and H. Y. Hwang, Superconductivity in an infinite-layer nickelate, Nature (London) **572**, 624 (2019).

[8] H. Sun, M. Huo, X. Hu, J. Li, Z. Liu, Y. Han, L. Tang, Z. Mao, P. Yang, B. Wang *et al.*, Signatures of superconductivity near

80 K in a nickelate under high pressure, Nature (London) **621**, 493 (2023).

[9] Y. Zhang, L.-F. Lin, A. Moreo, and E. Dagotto, Electronic structure, dimer physics, orbital-selective behavior, and magnetic tendencies in the bilayer nickelate superconductor $La_3Ni_2O_7$ under pressure, Phys. Rev. B **108**, L180510 (2023).

[10] Z. Ouyang, J.-M. Wang, J.-X. Wang, R.-Q. He, L. Huang, and Z.-Y. Lu, Hund electronic correlation in $La_3Ni_2O_7$ under high pressure, Phys. Rev. B **109**, 115114 (2024).

[11] Y. Gu, C. Le, Z. Yang, X. Wu, and J. Hu, Effective model and pairing tendency in bilayer Ni-based superconductor $La_3Ni_2O_7$, arXiv:2306.07275.

[12] V. Christiansson, F. Petocchi, and P. Werner, Correlated electronic structure of $La_3Ni_2O_7$ under pressure, Phys. Rev. Lett. **131**, 206501 (2023).

[13] F. Lechermann, J. Gondolf, S. Bötzel, and I. M. Eremin, Electronic correlations and superconducting instability in $La_3Ni_2O_7$ under high pressure, Phys. Rev. B **108**, L201121 (2023).

[14] H. Sakakibara, N. Kitamine, M. Ochi, and K. Kuroki, Possible high T_c superconductivity in $La_3Ni_2O_7$ under high pressure through manifestation of a nearly-half-filled bilayer Hubbard model, Phys. Rev. Lett. **132**, 106002 (2024).

[15] Q.-G. Yang, D. Wang, and Q.-H. Wang, Possible $s_{\pm}$-wave superconductivity in $La_3Ni_2O_7$, Phys. Rev. B **108**, L140505 (2023).

[16] Y. Shen, M. Qin, and G.-M. Zhang, Effective bi-layer model Hamiltonian and density-matrix renormalization group study for the high-T_c superconductivity in $La_3Ni_2O_7$ under high pressure, Chin. Phys. Lett. **40**, 127401 (2023).

[17] D. A. Shilenko and I. V. Leonov, Correlated electronic structure, orbital-selective behavior, and magnetic correlations in double-layer $La_3Ni_2O_7$ under pressure, Phys. Rev. B **108**, 125105 (2023).

[18] Z. Liu, M. Huo, J. Li, Q. Li, Y. Liu, Y. Dai, X. Zhou, J. Hao, Y. Lu, M. Wang *et al.*, Electronic correlations and energy gap in the bilayer nickelate $La_3Ni_2O_7$, arXiv:2307.02950.

[19] W. Wú, Z. Luo, D.-X. Yao, and M. Wang, Charge transfer and Zhang-Rice singlet bands in the nickelate superconductor $La_3Ni_2O_7$ under pressure, Sci. China Phys. Mech. Astron. **67**, 117402 (2024).

[20] Y. Cao and Y.-f. Yang, Flat bands promoted by Hund's rule coupling in the candidate double-layer high-temperature superconductor $La_3Ni_2O_7$ under high pressure, Phys. Rev. B **109**, L081105 (2024).

[21] X. Chen, P. Jiang, J. Li, Z. Zhong, and Y. Lu, Critical charge and spin instabilities in superconducting $La_3Ni_2O_7$, arXiv:2307.07154.

[22] Y.-B. Liu, J.-W. Mei, F. Ye, W.-Q. Chen, and F. Yang, The $s^{\pm}$-wave pairing and the destructive role of apical-oxygen deficiencies in $La_3Ni_2O_7$ under pressure, Phys. Rev. Lett. **131**, 236002 (2023).

[23] Y. Zhang, D. Su, Y. Huang, H. Sun, M. Huo, Z. Shan, K. Ye, Z. Yang, R. Li, M. Smidman *et al.*, High-temperature superconductivity with zero-resistance and strange metal behavior in $La_3Ni_2O_7$, arXiv:2307.14819.

[24] H. Oh and Y.-H. Zhang, Type-II $t-J$ model and shared superexchange coupling from Hund's rule in superconducting $La_3Ni_2O_7$, Phys. Rev. B **108**, 174511 (2023).

[25] Z. Liao, L. Chen, G. Duan, Y. Wang, C. Liu, R. Yu, and Q. Si, Electron correlations and superconductivity in $La_3Ni_2O_7$ under pressure tuning, Phys. Rev. B **108**, 214522 (2023).

[26] C. Lu, Z. Pan, F. Yang, and C. Wu, Interlayer coupling driven high-temperature superconductivity in $La_3Ni_2O_7$ under pressure, Phys. Rev. Lett. **132**, 146002 (2024).

[27] X.-Z. Qu, D.-W. Qu, J. Chen, C. Wu, F. Yang, W. Li, and G. Su, Bilayer t–J–$J_{\perp}$ model and magnetically mediated pairing in the pressurized nickelate $La_3Ni_2O_7$, Phys. Rev. Lett. **132**, 036502 (2024).

[28] Y. Zhang, L.-F. Lin, A. Moreo, T. A. Maier, and E. Dagotto, Structural phase transition, $s_{\pm}$-wave pairing and magnetic stripe order in the bilayered nickelate superconductor $La_3Ni_2O_7$ under pressure, Nat. Commun. **15**, 2470 (2024).

[29] Y.-f. Yang, G.-M. Zhang, and F.-C. Zhang, Minimal effective model and possible high-T_c mechanism for superconductivity of $La_3Ni_2O_7$ under high pressure, Phys. Rev. B **108**, L201108 (2023).

[30] K. Jiang, Z. Wang, and F.-C. Zhang, High temperature superconductivity in $La_3Ni_2O_7$, Chin. Phys. Lett. **41** 017402 (2024).

[31] Y. Zhang, L.-F. Lin, A. Moreo, T. A. Maier, and E. Dagotto, Trends of electronic structures and $s_{\pm}$-wave pairing for the rare-earth series in bilayer nickelate superconductor $R_3Ni_2O_7$, Phys. Rev. B **108**, 165141 (2023).

[32] J. Huang, Z. D. Wang, and T. Zhou, Impurity and vortex states in the bilayer high-temperature superconductor $La_3Ni_2O_7$, Phys. Rev. B **108**, 174501 (2023).

[33] J. Yang, H. Sun, X. Hu, Y. Xie, T. Miao, H. Luo, H. Chen, B. Liang, W. Zhu, G. Qu *et al.*, Orbital-dependent electron correlation in double-layer nickelate $La_3Ni_2O_7$, arXiv:2309.01148.

[34] S. Ryee, N. Witt, and T. O. Wehling, Critical role of interlayer dimer correlations in the superconductivity of $La_3Ni_2O_7$, arXiv:2310.17465.

[35] J. Chen, F. Yang, and W. Li, Orbital-selective superconductivity in the pressurized bilayer nickelate $La_3Ni_2O_7$: An infinite projected entangled-pair state study, arXiv:2311.05491.

[36] Z. Luo, B. Lv, M. Wang, W. Wú, and D.-X. Yao, High-T_c superconductivity in $La_3Ni_2O_7$ based on the bilayer two-orbital t-J model, arXiv:2308.16564.

[37] Z. Luo, X. Hu, M. Wang, W. Wú, and D.-X. Yao, Bilayer two-orbital model of $La_3Ni_2O_7$ under pressure, Phys. Rev. Lett. **131**, 126001 (2023).

[38] A. Georges, G. Kotliar, W. Krauth, and M. J. Rozenberg, Dynamical mean-field theory of strongly correlated fermion systems and the limit of infinite dimensions, Rev. Mod. Phys. **68**, 13 (1996).

[39] T. Maier, M. Jarrell, T. Pruschke, and M. H. Hettler, Quantum cluster theories, Rev. Mod. Phys. **77**, 1027 (2005).

[40] A. Georges, L. de' Medici, and J. Mravlje, Strong correlations from Hund's coupling, Annu. Rev. Condens. Matter Phys. **4**, 137 (2013).

[41] E. Koch, G. Sangiovanni, and O. Gunnarsson, Sum rules and bath parametrization for quantum cluster theories, Phys. Rev. B **78**, 115102 (2008).

[42] A. Foley, S. Verret, A.-M. S. Tremblay, and D. Sénéchal, Coexistence of superconductivity and antiferromagnetism in the Hubbard model for cuprates, Phys. Rev. B **99**, 184510 (2019).

[43] M. Caffarel and W. Krauth, Exact diagonalization approach to correlated fermions in infinite dimensions: Mott transition and superconductivity, Phys. Rev. Lett. **72**, 1545 (1994).

[44] R.-Q. He and Z.-Y. Lu, Quantum renormalization groups based on natural orbitals, Phys. Rev. B **89**, 085108 (2014).

[45] R.-Q. He, J. Dai, and Z.-Y. Lu, Natural orbitals renormalization group approach to the two-impurity Kondo critical point, Phys. Rev. B **91**, 155140 (2015).

[46] J.-M. Wang, Y. Chen, Y.-H. Tian, R.-Q. He, and Z.-Y. Lu, Solving multiorbital dynamical mean-field theory using natural orbitals renormalization group, arXiv:2209.14178.

[47] L.-F. Lin, Y. Zhang, G. Alvarez, A. Moreo, and E. Dagotto, Origin of insulating ferromagnetism in iron oxychalcogenide $Ce_2O_2FeSe_2$, Phys. Rev. Lett. **127**, 077204 (2021).

[48] F. B. Kugler and G. Kotliar, Is the orbital-selective Mott phase stable against interorbital hopping? Phys. Rev. Lett. **129**, 096403 (2022).